Supplement of Biogeosciences, 23, 1365–1381, 2026
https://doi.org/10.5194/bg-23-1365-2026-supplement
© Author(s) 2026. CC BY 4.0 License.

Supplement of

Phenology, fluxes and their drivers in major Indian agroecosystems: A modeling study using the Community Land Model (CLM5)

Kangari Narender Reddy and Somnath Baidya Roy

Correspondence to: Kangari Narender Reddy (n.kangari@reading.ac.uk)

The copyright of individual parts of the supplement might differ from the article licence.

S1. Carbon fluxes in CLM5 for C3 crops

Photosynthesis in C_3 plants is based on the model of Farquhar et al. (1980). In its simplest form, leaf net photosynthesis after accounting for dark respiration (R_d) is:

$$A_n = min\,(A_c, A_j, A_p) - R_d$$

$$A_c = \frac{V_{c\,max}(c_i - \Gamma)}{c_i + K_c(1 + o_i/K_o)}$$

$$A_j = \frac{J_x(c_i - \Gamma)}{4c_i + 8\Gamma}$$

$$A_p = 3T_p$$

where A_c (μ mol CO_2 m^{-2} s^{-1}) is the RuBP carboxylase (Rubisco) limited rate of carboxylation, A_j (μ mol CO_2 m^{-2} s^{-1}) is the maximum rate of carboxylation allowed by the capacity to regenerate RuBP (i.e., the light-limited rate), and A_p (μ mol CO_2 m^{-2} s^{-1}) is the product-limited rate of carboxylation for C_3 plants. In these equations, c_i is the internal leaf CO_2 partial pressure (Pa), and $o_i = 0.20P_{atm}$ is the O_2 partial pressure (Pa). K_c and K_o are the Michaelis-Menten constants (Pa) for CO_2 and O_2. Γ (Pa) is the CO_2 compensation point. $V_{c\,max}$ is the maximum rate of carboxylation (µmol m^{-2} s^{-1}), and J_x is the electron transport rate (µmol m^{-2} s^{-1}). T_p is the triose phosphate utilization rate (µmol m^{-2} s^{-1}), taken as $T_p = 0.167Vc$ max so that $A_p = 0.5Vc$ max for C_3 plants (as in Collatz et al. 1992). For more details on the calculation of V_{cmax}, J_x, T_p, K_c, K_o, and Γ at various temperatures, please refer to CLM5 Tech Note: Chapter 9, and for information on respiration, refer to CLM5 Tech Note: Chapter 17 (Lawrence et al., 2018).

S2. Improvement of Indian crop physiology in Reddy et al. (2025)

For example, the bias in the LAI simulation was 0.81 and 0.66 for wheat and rice in the default model. The bias in LAI reduced in the improved model to 0.43 and 0.34 for wheat and rice (Reddy et al., 2025). The largest improvement in crop simulation was observed in wheat growing season length, RMSE improved from 63 days in the default case to 15 days in CLM5_Mod2 (Reddy et al., 2025). The site scale observation data from 2000 to 2014 was used for comparing the crop physiology simulation by various versions of the CLM5 model in Reddy et al. (2025).

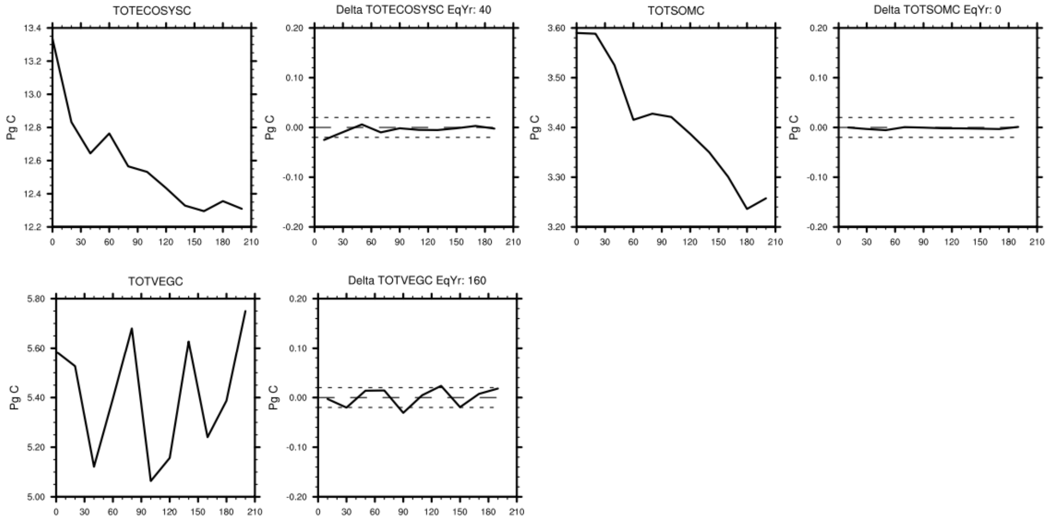

Figure S1: The spinup of the CLM5 model for 200 years in the accelerated mode and the evolution to reach equilibrium for variables: TOTECOSYSC- Total Ecosystem Carbon, TOTSOMC- Total Soil Carbon Organic Matter, and TOTVEGC- Total Vegetative Carbon.

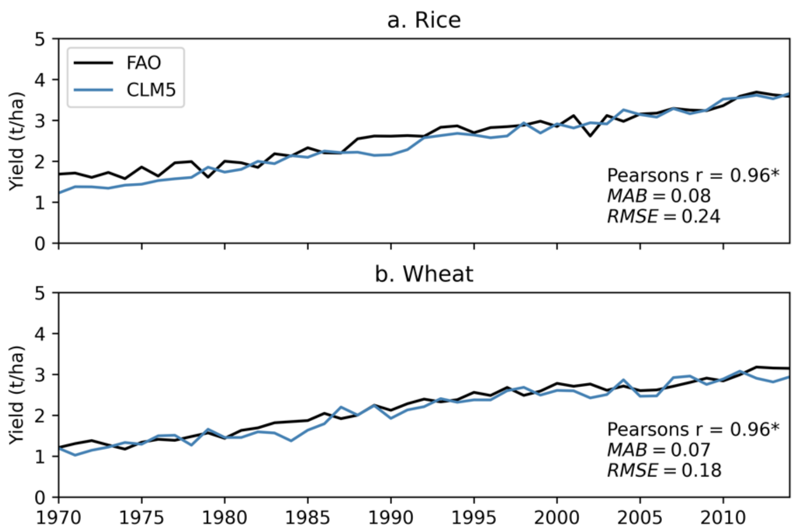

Figure S2: Comparison of yield simulated by CLM5 for major Indian crops (a) Rice and (b) Wheat against the FAO observations

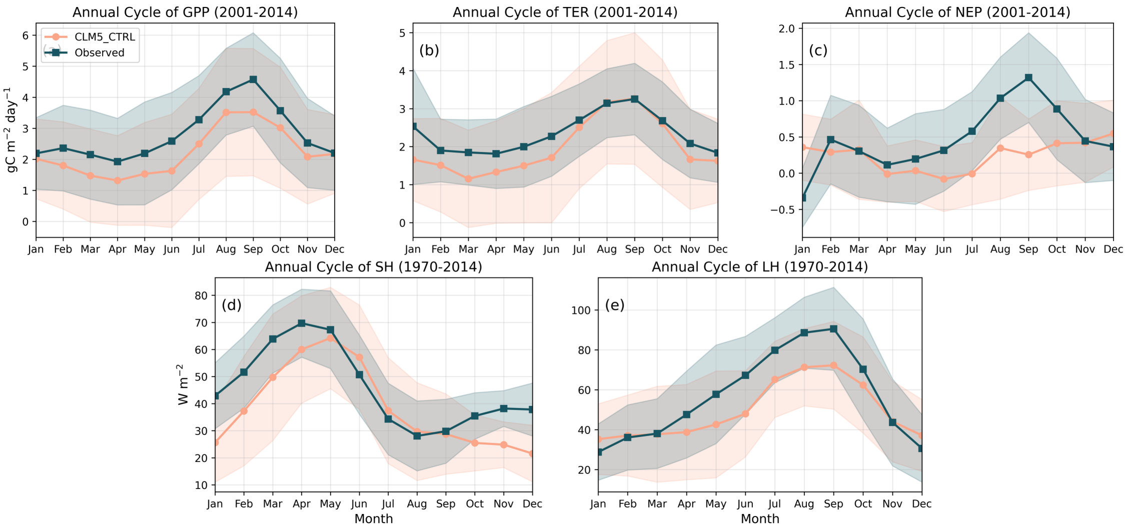

Figure S3: Mean seasonal cycles of carbon and energy fluxes simulated by CLM5 and fluxes from observations. Panels show the climatological annual cycles of (a) gross primary production (GPP), (b) total ecosystem respiration (TER), and (c) net ecosystem production (NEP) for the period 2001–2014, and of (d) sensible heat flux (SH) and (e) latent heat flux (LH) for the period 1970–2014. Solid lines indicate monthly means simulated by CLM5 and derived from FLUXCOM observations. Shaded envelopes represent ±1 standard deviation of the monthly fluxes for CLM5 and observations.

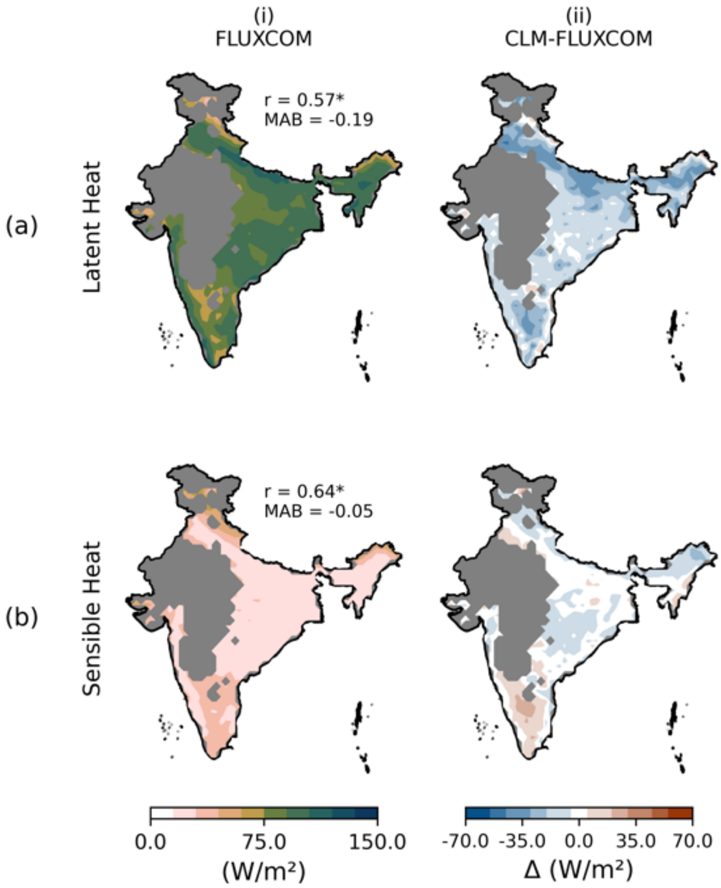

Figure S4: (a) Latent Heat, and (b) Sensible Heat from (i) FLUXCOM data, and (ii) The difference between CLM5 and FLUXCOM data. All plots are for the rice-growing regions (grid cells with more than 10% of land area covered by rice crop) and the mean of the data growing season (July to October). All fluxes are monthly means over the period 1970 to 2014.

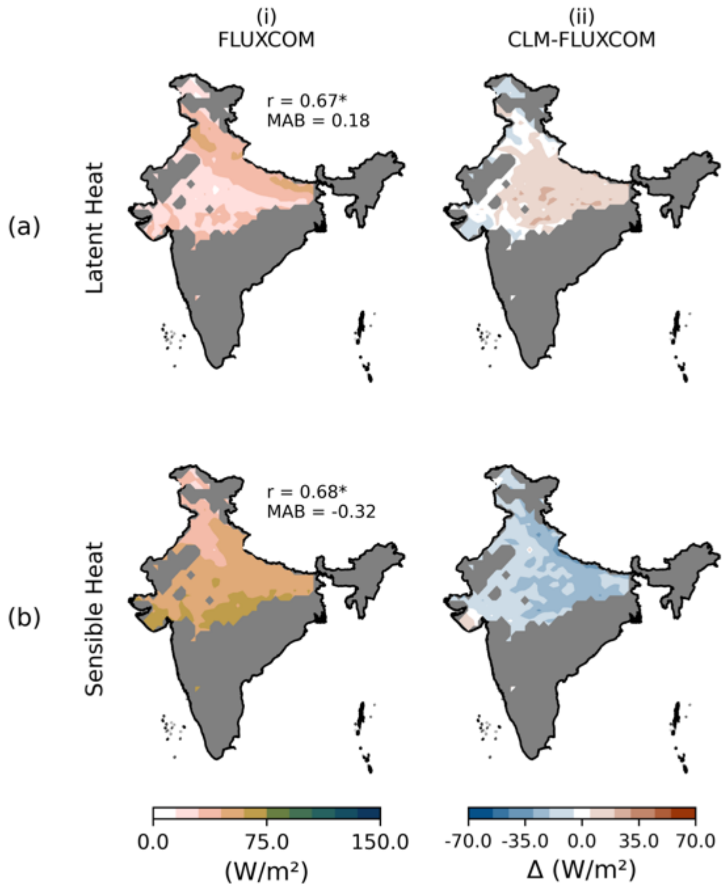

Figure S5: (a) Latent Heat, and (b) Sensible Heat from (i) FLUXCOM data, and (ii) The difference between CLM5 and FLUXCOM data. All plots are for the wheat-growing regions (grid cells with more than 10% of land area covered by wheat crop) and the mean of the growing season (December to March). All fluxes are monthly means over the period 1970 to 2014.

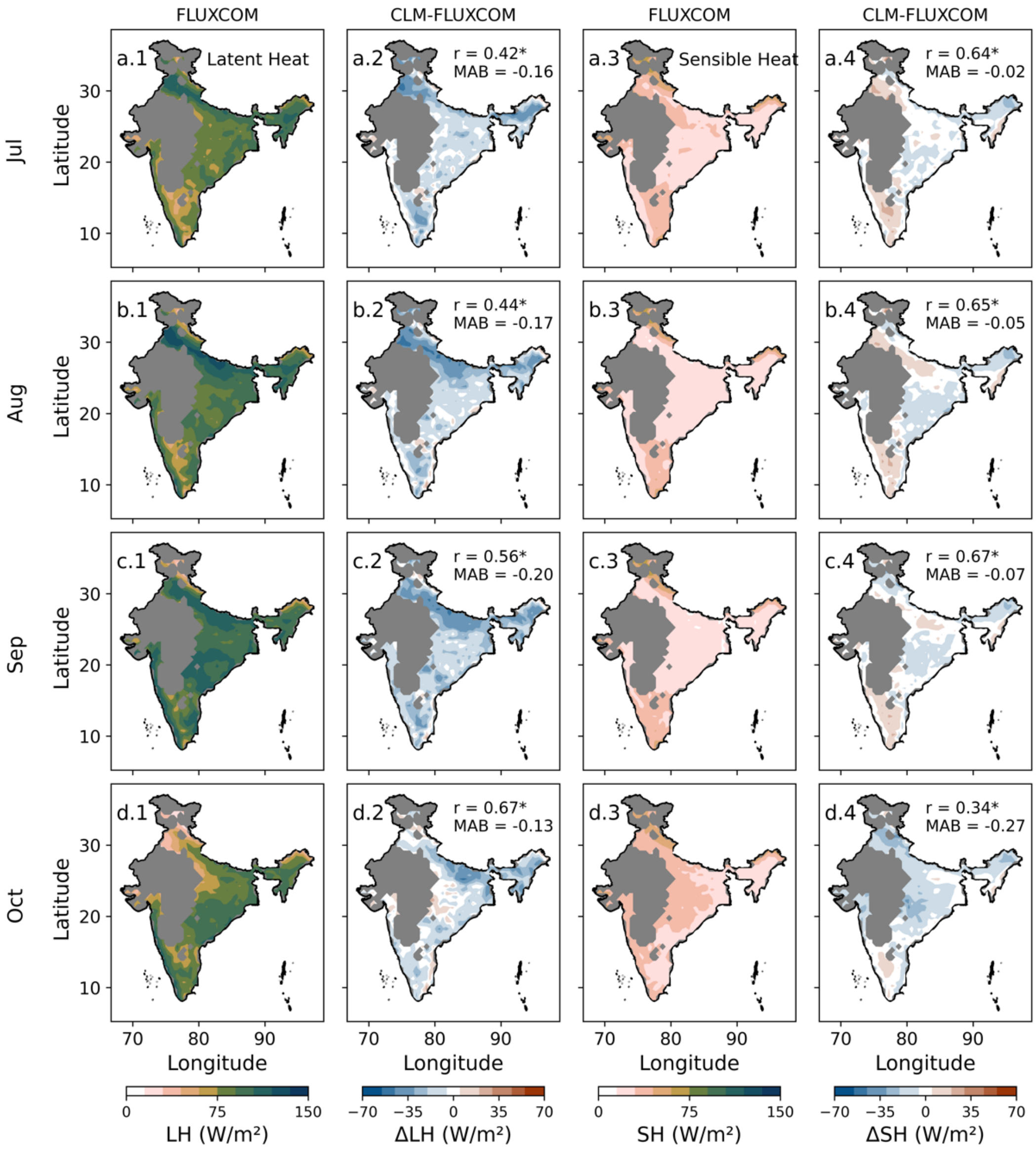

Figure S6: Comparison of monthly water and energy fluxes simulated by CLM5 CTRL run against the FLUXCOM data during the rice growing season, July to October. The area shown here is a region with more than 10% of the land area covered by rice. The second and fourth columns show the difference between CLM5 and FLUXCOM latent and sensible heat, respectively. The monthly mean fluxes over the period 1970-2014 are shown here. Pearson *r* in the plots is tested for significance, and values that are significant have an asterisk '*'.

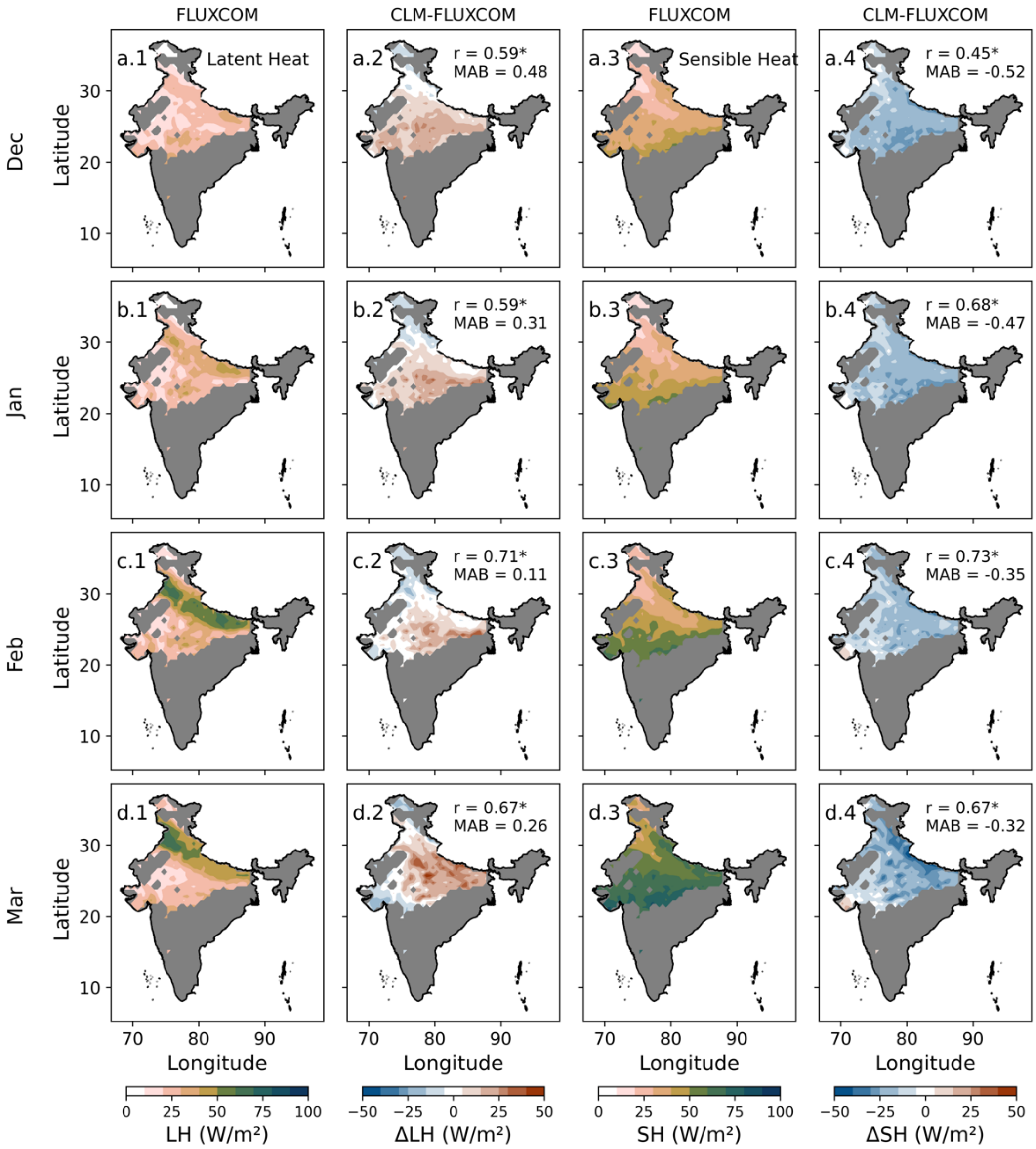

Figure S7: Comparison of monthly water and energy fluxes simulated by CLM5 CTRL run against the FLUXCOM data during the wheat growing season, December to March. The area shown here is a region with more than 10% of the land area covered by wheat. The second and fourth columns show the difference between CLM5 and FLUXCOM latent and sensible heat, respectively. The monthly mean fluxes over the period 1970-2014 are shown here. Pearson *r* in the plots is tested for significance, and values that are significant have an asterisk '*'.

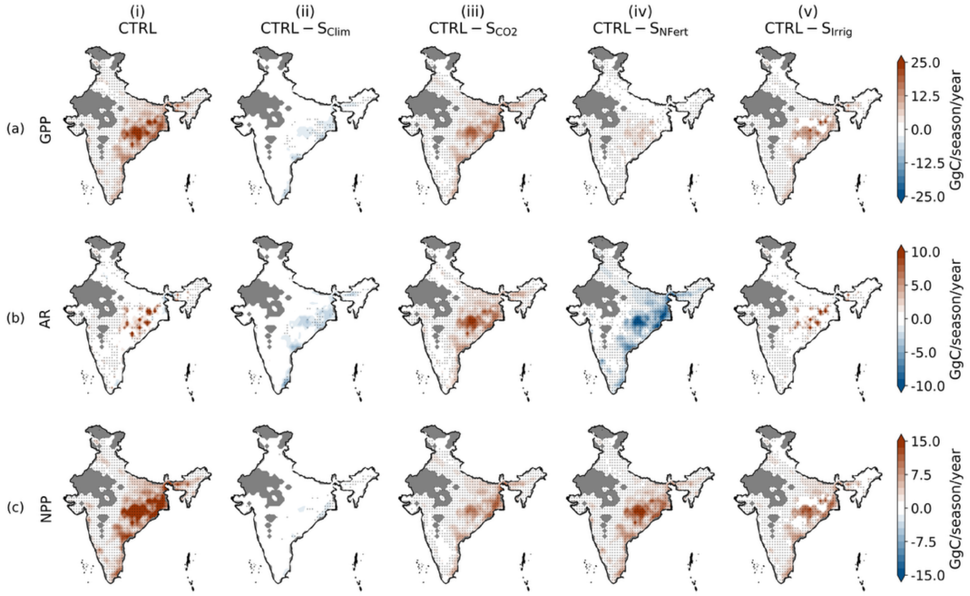

Figure S8: Spatial trend observed in carbon fluxes (a.) GPP, (b.) AR, and (c.) NPP in rice-growing regions in the (i) CTRL simulation. (ii) to (v) show the impact of each driver. Regions stippled implies the trend is statistically significant at p<0.05.

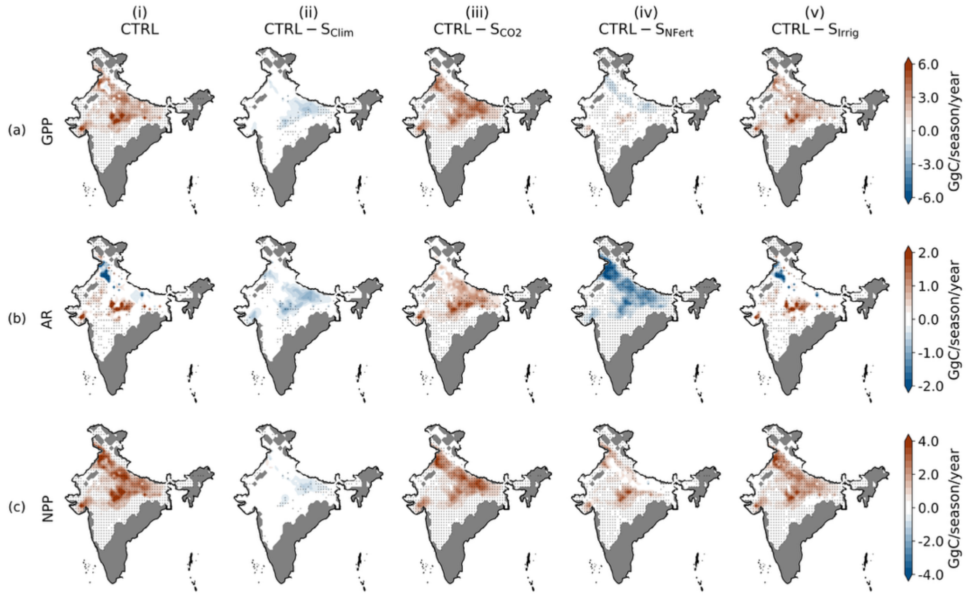

Figure S9: Spatial trend observed in carbon fluxes (a) GPP, (b) AR, and (c) NPP of wheat-growing regions in the (i) CTRL simulation. (ii) to (v) show the impact of each driver. Regions stippled implies the trend is statistically significant at p<0.05.

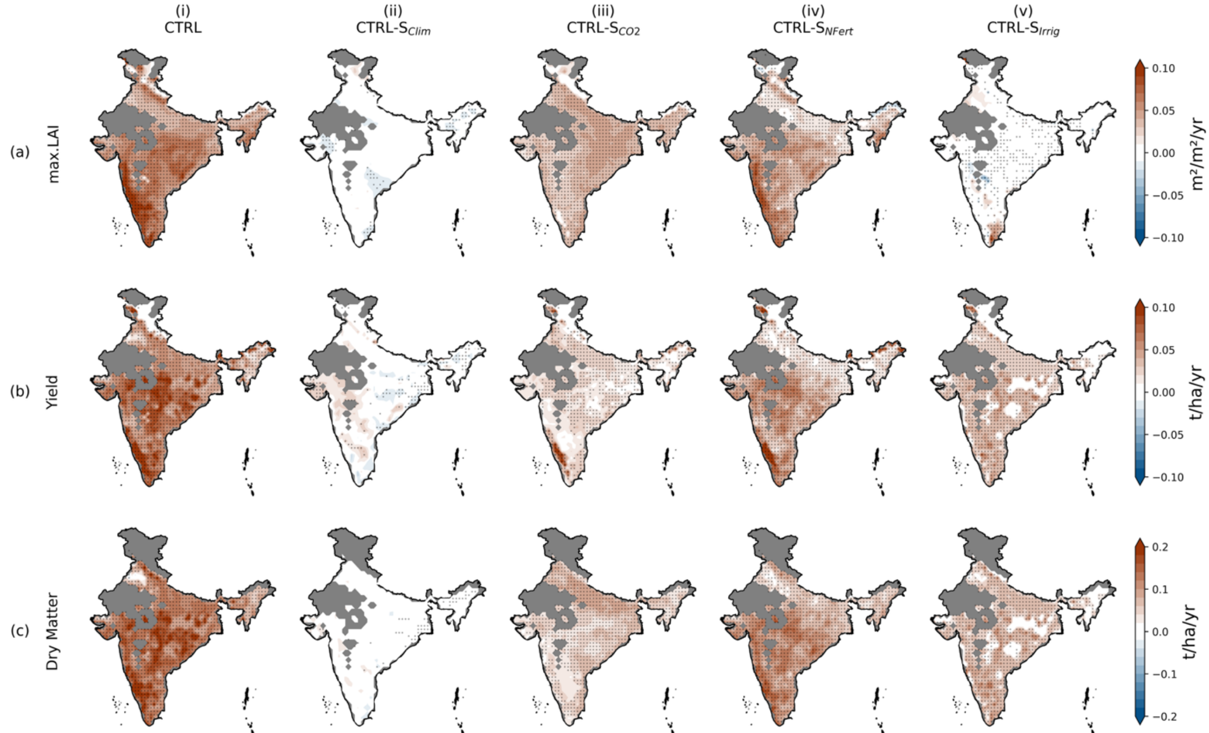

Figure S10: Spatial trend observed in (a) max. LAI, (b) Yield, and (c) Dry Matter of rice-growing regions in the (i) CTRL simulation. (ii) to (v) shows the impact of each driver. Regions stippled implies the trend is statistically significant at $p<0.05$.

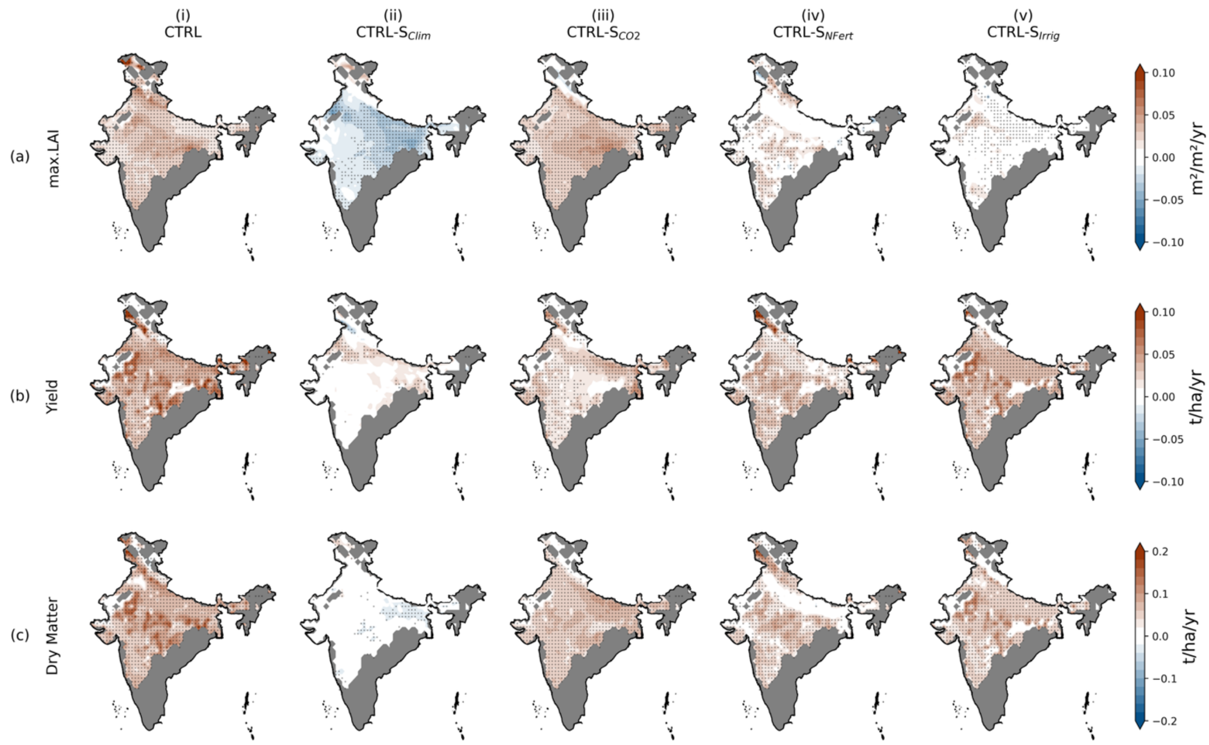

Figure S11: Spatial trend observed in (a) max. LAI, (b) Yield, and (c) Dry Matter of wheat-growing regions in the (i) CTRL simulation. (ii) to (v) shows the impact of each driver. Regions stippled implies the trend is statistically significant at $p<0.05$.

Table S1: Comparing GPP simulated by CLM5 for rice and wheat against other studies

	Location	GPP (gC/m^2)	AR/GPP	Reference
Rice	International Rice Research Institute, Philippines	1192 1464	0.67	Alberto et al., 2009
	Mase paddy site, Japan	1140	0.65	Saito et al., 2005
	Central Rice Research Institute, Cuttak, India	811	0.44	Bhattacharya et al., 2013
	Bangladesh Agricultural University Farmland, Dhaka, Bangladesh	1312 1574	0.58 0.52	Hossen et al., 2011
	North China Plain, China	987 966	0.56 0.56	Chen et al., 2015
	Indian Agricultural Research Institute, New Delhi, India	753	0.51	Kumar et al., 2021
	Rice growing region of India	1528.3 ± 561	0.53 ± 0.05	This study
Wheat	Selhausen test site, Germany (First Year)	1304	0.51	Schmidt et al., 2012
	Selhausen test site, Germany (Second Year)	1067	0.49	Schmidt et al., 2012
	North China Plain, China	1220 1135 859	0.52 0.54 0.53	Chen et al., 2015
	Saharanpur, India	1024	-	Patel et al., 2021
	Indian Agricultural Research Institute, New Delhi, India	888	0.34	Kumar et al., 2021
	Wheat growing regions of India	862.6 ± 438.6	0.42 ± 0.04	This study

References:

Alberto, M. C. R., Wassmann, R., Hirano, T., Miyata, A., Kumar, A., Padre, A., and Amante, M.: CO2/heat fluxes in rice fields: Comparative assessment of flooded and non-flooded fields in the Philippines, Agr. Forest Meteorol., 149, 1737–1750, https://doi.org/10.1016/j.agrformet.2009.06.003, 2009.

Bhattacharyya P., Neogi S., Roy K. S., Dash P. K., Tripathi R., and Rao K. S.: Net ecosystem CO2 exchange and carbon cycling in tropical lowland flooded rice ecosystem. Nutr. Cycl. Agroecosyst., 95:133–144, https://doi.org/10.1007/s10705-013-9553-1, 2013.

Chen, C., Dan, L.I., Zhiqiu, G., Tang, J., Xiaofeng, G., Linlin, W., and Bingcheng, W.: Seasonal and interannual variations of carbon exchange over a rice-wheat rotation system on the north China plain, Advan. Atmos. Sci., 32, 1365–1380, https://doi.org/10.1007/s00376-015-4253-1, 2015.

Farquhar, G.D., von Caemmerer, S.V. and Berry, J.A.: A biochemical model of photosynthetic CO 2 assimilation in leaves of C 3 species. planta, 149, pp.78-90, https://doi.org/10.1007/BF00386231, 1980.

Hossen, M. S., Mano, M., Miyata, A., Baten, M. A., and Hiyama, T.: Seasonality of ecosystem respiration in a double-cropping paddy field in Bangladesh, Biogeosciences Discuss., 8, 8693–8721, https://doi.org/10.5194/bgd-8-8693-2011, 2011.

Kumar, A., Bhatia, A., Sehgal, V. K., Tomer, R., Jain, N., and Pathak, H.: Net Ecosystem Exchange of Carbon Dioxide in Rice-Spring Wheat System of Northwestern Indo-Gangetic Plains, Land, 10, 701, https://doi.org/10.3390/land10070701, 2021.

Lawrence, D. M., Fisher, R., Koven, C., Oleson, K., Svenson, S., Vertenstein, M. (coordinating lead authors), Andre, B., Bonan, G., Ghimire, B., van Kampenhout, L., Kennedy, D., Kluzek, E., Knox, R., Lawrence, P., Li, F., Li, H., Lombardozzi, D., Lu, Y., Perket, J., Riley, W., Sacks, W., Shi, M., Wieder, W., Xu, C. (lead authors), Ali, A., Badger, A., Bisht, G., Broxton, P., Brunke, M., Buzan, J., Clark, M., Craig, T., Dahlin, K., Drewniak, B., Emmons, L., Fisher, J., Flanner, M., Gentine, P., Lenaerts, J., Levis, S., Leung, L. R., Lipscomb, W., Pelletier, J., Ricciuto, D., M., Sanderson, B., Shuman, J., Slater, A., Subin, Z., Tang, J., Tawfik, A., Thomas, Q., Tilmes, S., Vitt, F., and Zeng, X.: Technical Description of version 5.0 of the Community Land Model (CLM), Natl. Cent. Atmospheric Res. (NCAR), available at http://www.cesm.ucar.edu/models/cesm2/land/CLM50_Tech_Note.pdf (last access: 08 July 2024), 2018.

Patel, N. R., Pokhariyal, S., Chauhan, P., and Dadhwal, V. K.: Dynamics of CO2 fluxes and controlling environmental factors in sugarcane (C4)–wheat (C3) ecosystem of dry sub-humid region in India, Int. J. Biometeorol., 65, 1069–1084, https://doi.org/10.1007/s00484-021-02088-y, 2021.

Saito, M., Miyata, A., Nagai, H. and Yamada, T.: Seasonal variation of carbon dioxide exchange in rice paddy field in Japan. Agric. For. Meteorol., 135(1-4), pp.93-109, https://doi.org/10.1016/j.agrformet.2005.10.007, 2005.

Schmidt, M., Reichenau, T.G., Fiener, P. and Schneider, K.: The carbon budget of a winter wheat field: An eddy covariance analysis of seasonal and inter-annual variability, Agric. For. Meteorol., 165, pp.114-126, https://doi.org/10.1016/j.agrformet.2012.05.012, 2012.